J Paleolimnol (2009) 41:189–208
DOI 10.1007/s10933-008-9261-z

ORIGINAL PAPER

Late Holocene storm-trajectory changes inferred from the oxygen isotope composition of lake diatoms, south Alaska

Caleb J. Schiff · Darrell S. Kaufman · Alexander P. Wolfe · Justin Dodd · Zachary Sharp

Received: 10 April 2008 / Accepted: 12 September 2008 / Published online: 14 October 2008

Abstract The oxygen isotope ratios of diatoms ($\delta^{18}O_{diatom}$), and the oxygen and hydrogen isotope ratios of lake water (δW) of lakes in south Alaska provide insight into past changes in atmospheric circulation. Lake water was collected from 31 lakes along an elevation transect and diatoms were isolated from lake sediment from one lake (Mica Lake) in south Alaska. In general, δW values from coastal lakes overlap the global meteoric water line (GMWL). δW values from interior lakes do not lie on the GMWL; they fall on a local evaporation line trajectory suggesting source isotopes are depleted with respect to maritime lakes. Sediment cores were recovered from 58 m depth in Mica Lake (60.96° N, 148.15° W; 100 m asl), an evaporation-insensitive lake in the western Prince William Sound. Thirteen calibrated ^{14}C ages on terrestrial macrofossil samples were used to construct an age-depth model for core MC-2, which spans 9910 cal years. Diatoms from 46, 0.5-cm-thick samples were isolated and analyzed for their oxygen isotope ratios. The analyses employed a newly designed, stepwise fluorination technique, which uses a CO_2 laser-ablation system, coupled to a mass spectrometer, and has an external reproducibility of ±0.2‰. $\delta^{18}O_{diatom}$ values from Mica Lake sediment range between 25.2 and 29.8‰. $\delta^{18}O_{diatom}$ values are relatively uniform between 9.6 and 2.6 ka, but exhibit a four-fold increase in variability since 2.6 ka. High-resolution sampling and analyses of the top 100 cm of our lake cores suggest large climate variability during the last 2000 years. The 20th century shows a +4.0‰ increase of $\delta^{18}O_{diatom}$ values. Shifts of $\delta^{18}O_{diatom}$ values are likely not related to changes in diatom taxa or dissolution effects. Late Holocene excursions to lower $\delta^{18}O_{diatom}$ values suggest a reduction of south-to-north storm trajectories delivered by meridional flow, which likely corresponds to prolonged intervals when the Aleutian Low pressure system weakened. Comparisons with isotope records of precipitation (δP) from the region support the storm-

This is one of fourteen papers published in a special issue dedicated to reconstructing late Holocene climate change from Arctic lake sediments. The special issue is a contribution to the International Polar Year and was edited by Darrell Kaufman.

C. J. Schiff · D. S. Kaufman (✉)
Department of Geology, Northern Arizona University, Flagstaff, AZ 86011-4099, USA
e-mail: darrell.kaufman@nau.edu

C. J. Schiff
e-mail: caleb.schiff@nau.edu

A. P. Wolfe
Department of Earth and Atmospheric Sciences, University of Alberta, Edmonton, AB, Canada T6G 2E3
e-mail: awolfe@ualberta.ca

J. Dodd · Z. Sharp
Department of Earth and Planetary Sciences, University of New Mexico, Albuquerque, NM 87131-0001, USA
e-mail: jpd829@unm.edu

Z. Sharp
e-mail: zsharp@unm.edu

track hypothesis, and add to evidence for variability in North Pacific atmospheric circulation during the Holocene.

Keywords Oxygen isotopes · Holocene climate change · Aleutian Low · Diatoms · North Pacific · Alaska

Introduction

The oxygen and hydrogen isotope composition of lake water (δW) integrates spatial and temporal changes in climate on a variety of scales. Where precipitation rates are high, lakes are spatially dense and δW commonly reflects the isotopes of precipitation (δP), which is strongly correlated with environmental variables (Dansgaard 1964). Minerals and organic matter that form in isotopic equilibrium with lake water, and are preserved in lake sediment, can be an excellent archive for interpreting past regional climate change. Numerous components of lake sediment have been investigated for reconstructing δW in Alaska and elsewhere, including: chironomid head capsules (e.g. Wooller et al. 2004), aquatic cellulose (e.g. Sauer et al. 2001), and authigenic carbonate (e.g. Hu et al. 2001; Anderson et al. 2005). All of these materials have limitations, however. For example, authigenic carbonate studies are limited to alkaline lakes, and aquatic cellulose may not be preserved continuously (e.g. Sauer et al. 2001). Recently, the oxygen isotope composition of lake diatoms ($\delta^{18}O_{diatom}$) has emerged as an alternate proxy of paleo δW (see review by Leng and Barker 2006). Diatoms are ubiquitous in most lakes and their silica structure is well preserved in non-alkaline lakes. Recent advances in diatom separation (Rings et al. 2004) and dehydroxylation techniques (Dodd et al. 2007) have expanded the method to lakes with relatively low diatom concentrations.

In this study, we investigate the oxygen isotope composition of water and diatoms from south Alaskan lakes and their watersheds (Fig. 1). Our study reveals large spatial and temporal variability of δW and $\delta^{18}O_{diatom}$. The modern δW data span three climate regimes and the temporal record of $\delta^{18}O_{diatom}$ from one site (Mica Lake) extends to 9600 cal BP. By sampling the core at higher resolution in the top 100 cm, our record provides greater detail of $\delta^{18}O_{diatom}$ changes during the last 2000 years. δW in lakes of maritime south Alaska reflects δP, whereas interior lakes are strongly affected by evaporation. The current understanding of δP in the North Pacific region does not allow a simple interpretation of the sedimentary $\delta^{18}O_{diatom}$ record from Mica Lake, but multiple controls are considered. We suggest that δP in south Alaska is strongly dictated by storm trajectories and therefore δW is controlled by large-scale changes of North Pacific atmospheric circulation. Specifically, the strength and position of the Aleutian Low pressure system is suggested as the main control of δP in south Alaska.

Reconstructing the low-frequency variability in the climatological Aleutian Low prior to the instrumental period is important because this major feature of ocean-atmospheric circulation strongly influences the climate of the North Pacific (Trenberth and Hurrell 1994; Rupper et al. 2004; Overland et al. 1999), and is predicted to intensify and shift northward under global warming (Salathé 2006). The hydroclimate of south Alaska is strongly influenced by variability in the Aleutian Low. The mass balance of glaciers (e.g. Hodge et al. 1998), organic matter in lake sediment (e.g. McKay 2007), abundance of far-traveled pollen (Spooner et al. 2003), accumulation rate in ice cores from Mt. Logan (Rupper et al. 2004), and the effective moisture in interior Yukon (Anderson et al. 2005) have all been interpreted as variability in the Aleutian Low on decadal to millennial time scales.

Study site

In south Alaska, winter surface air temperature and precipitation are largely determined by the strength and position of the Aleutian Low, a low-pressure system that steers wintertime storms inland to south Alaska (Fig. 2a). Rodionov et al. (2005) reviewed the meteorological expression of the ten strongest and ten weakest Aleutian Low years between 1951 and 2000 in the North Pacific (Fig. 2a). During years when the Aleutian Low is weak, it is split into two centers, one in the Gulf of Alaska and one east of Kamchatka. In the Gulf of Alaska, storms come from the west and northwest during weak Aleutian Low years, and from the southwest during strong Aleutian Low years. The increased southerly flow into the Gulf of Alaska

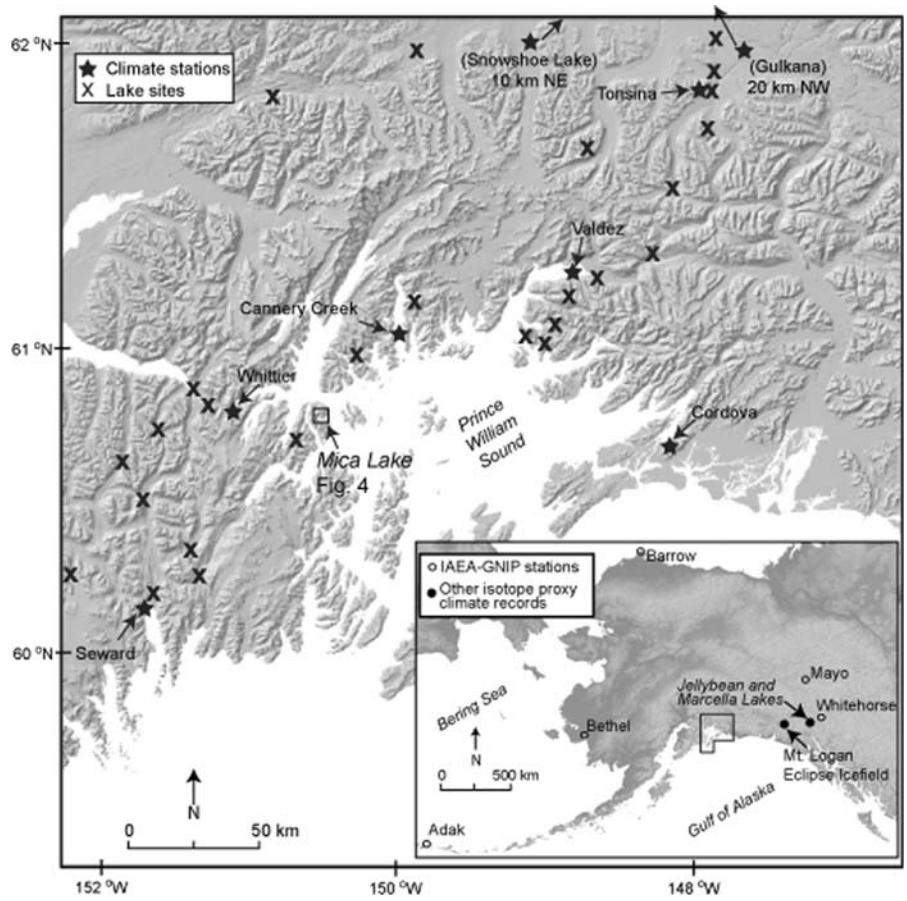

Fig. 1 Study area with water sampling sites (**X**), climate stations (★), North Pacific International Atomic Energy Agency-Global Network of Isotopes in Precipitation (IAEA-GNIP) stations (◯), locations of North Pacific paleorecords of stable isotopes of precipitation discussed in this paper (●), and Mica Lake

brings warm, moist air inland, which is well recorded at climate stations in south-central Alaska (Fig. 2b). Inverse (cold and dry) conditions occur farther west in the Aleutian Islands during strong Aleutian Low years. Farther north at Anchorage, winter precipitation does not increase much, but average temperatures are +5°C warmer during strong Aleutian Low years (Fig. 2b).

To provide a regional climate summary, data from long-term climate stations in Prince William Sound were used to calculate monthly averages (Fig. 3). All data were obtained from the Western Regional Climate Center of the Desert Research Institute (http://www.wrcc.dri.edu/index.html; last accessed 24 September 2007). Only sites with >90% of data for the period 1980–2005 were used, which limited the number of sites to five: Seward, Whittier, Cannery Creek, Valdez, and Cordova (Fig. 1). Prince William Sound receives the highest monthly precipitation rate during September (366 mm) and December (347 mm). The warmest (+13.2°C) and coldest (+3.2°C) months are July and January, respectively (Fig. 3a). Using the same data-screening criteria, data from three interior sites, Gulkana, Snowshoe Lake, and Tonsina were compared with the Prince William Sound sites. At the interior sites, precipitation is highest in July (44 mm) and August (36 mm). The warmest (+13.2°C) and coldest (−20.1°C) months are July and January, respectively (Fig. 3b). The strong climate gradient is evidenced by reduced precipitation and increased temperature range at the interior sites.

Mica Lake (informal name, 60.96° N, 148.15° W; 100 m asl) is located on Culross Island in the western Prince William Sound of southern Alaska, about 29 km east-southeast of Whittier (Fig. 1). Mica Lake was selected because the high precipitation rate in the Prince William Sound (>3 m year^{-1}) limits evaporation and the relatively warm setting promotes productivity of diatoms. The lake is hydrologically open with numerous small inflows and one outflow, which drains into a pond ~30 m below, then to the

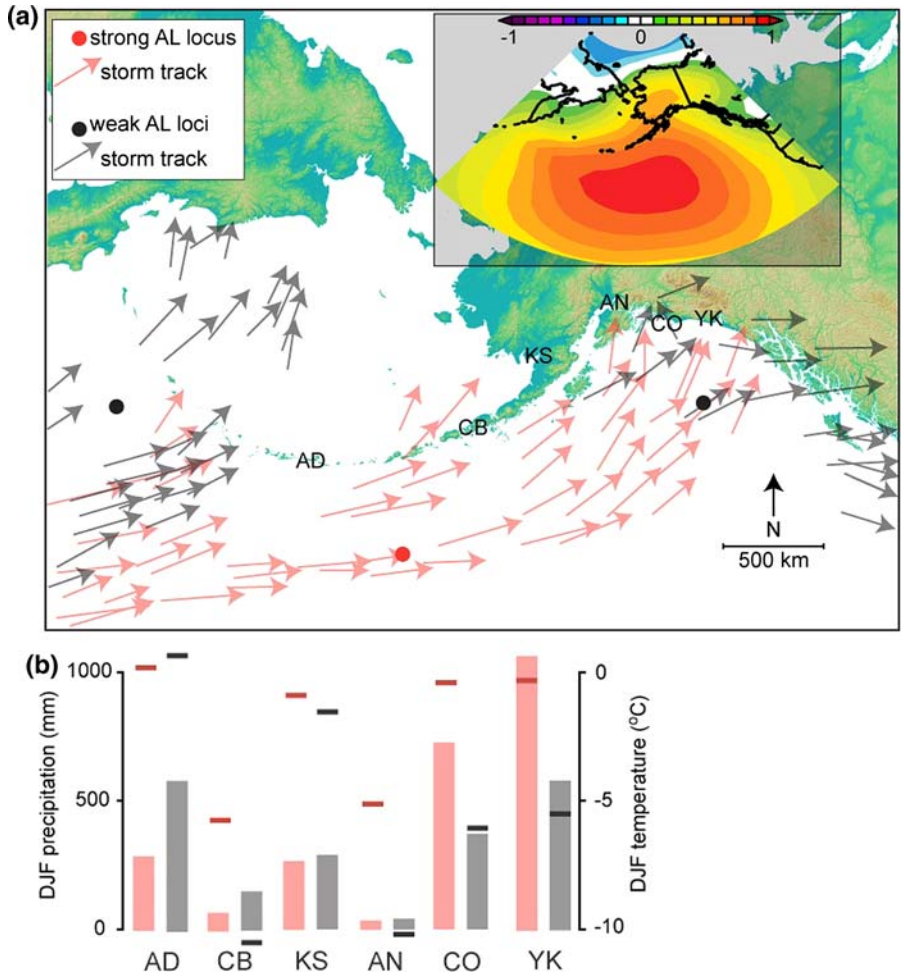

Fig. 2 **a** Comparison of storm track locations for the winter-time (DJF) Aleutian Low (AL) during the ten strongest (red) versus the ten weakest (black) years between 1951 and 2000 as summarized by Rodionov et al. (2005). Inset map illustrates the correlation between the North Pacific Index and the surface sea-level pressure during the winter months (DJF) between 1958 and 2005 from the NCEP/NCAR reanalysis dataset (Kalnay et al. 1996). **b** Summary of meteorological observations during the ten strongest and weakest Aleutian Low years at Adak (AD), Cold Bay (CB), King Salmon (KS), Anchorage (AN), Cordova (CO), and Yakutat (YK), displayed from left to right, respectively. Total DJF precipitation amounts are vertical bars, and average DJF temperatures are thick lines. In general, eastern sites record higher winter (DJF) precipitation and temperatures during strong Aleutian Low years. Precipitation amounts at Adak and Cold Bay are inversely related with eastern sites (Cordova and Yakutat). Precipitation amounts at King Salmon and Anchorage are nearly identical between strong and weak Aleutian Low years. Adak temperatures are inversely related to all other sites, although the difference between strong and weak years is small (+1.2°C). Climate data obtained from the Global Historic Climate Network (Vose et al. 1992)

coast (Fig. 4). The lake is at least 60 m deep, with surface and drainage areas of 0.8 and 4.0 km^2, respectively. Surface water pH was 6.0 and 6.2, and secchi-disk depth was 11.2 and 13.6 m, during June 2006 and August 2007, respectively.

Mica Lake fills a glacially over-deepened basin in a granite stock surrounded by meta-sedimentary rocks (Beikman 1980). The granite contains abundant mica, which forms a distinctive component of the sediment. Steep slopes surrounding most of the lake rise to summits 600 m asl within about 1 km of the lake (Fig. 4). The steep slopes are prone to snow avalanches and weathered debris that accumulates on the impermeable granite substrate is frequently flushed into the lake during high-precipitation events. The modern vegetation is Pacific coast forest (Ager 1998). Sitka spruce (*Picea sitchensis*) arrived ~2.5 ka and mountain hemlock (*Tsuga mertensiana*), the dominant

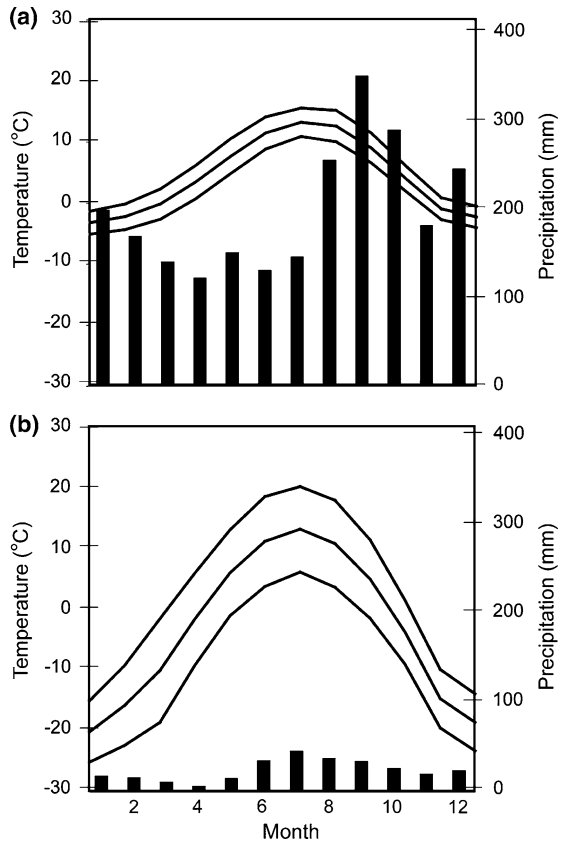

Fig. 3 Monthly maximum, mean, and minimum temperatures (solid lines), and precipitation (vertical bars) from five long-term climate stations around (**a**) Prince William Sound and (**b**) three interior stations between 1980 and 2005. Both climate summaries are plotted on equivalent axes. See text and Fig. 1 for climate station locations and explanation of data treatment

tree in the Mica Lake watershed, arrived soon after (Heusser 1983).

Materials and methods

Regional water sampling and isotope analyses

Lakes sampled for isotope analyses span three climate regimes of southern Alaska: maritime, transition, and interior (Papineau 2001). They are within 210 km of Mica Lake and range in elevation from 9 to 1160 m asl. (Table 1; Fig. 1). The Chugach Mountains, rising 4000 m and spanning about 500 km, form an effective moisture barrier, creating steep temperature and precipitation gradients across zones. In general, the maritime zone receives higher precipitation (2920 mm $year^{-1}$) and has lower seasonal temperature variations (from −3.2 to +13.2°C) compared to the interior zone (270 mm $year^{-1}$ and from −20.1 to +13.2°C) (Fig. 3). Both hydrologically open and closed (i.e. limited surface water input and outflow), as well as glacially-fed and non-glacial lakes, were sampled in nearly all climate zones (Table 1).

Water samples were collected from lakes, streams, precipitation, glaciers, and snowpacks across south-central Alaska during the summers of 2006 and 2007 (Fig. 1). Water samples were collected in 15-ml polyethelene bottles with little or no headspace, and sealed with vinyl tape. Lake surface waters were collected from the approximate center of the lake or

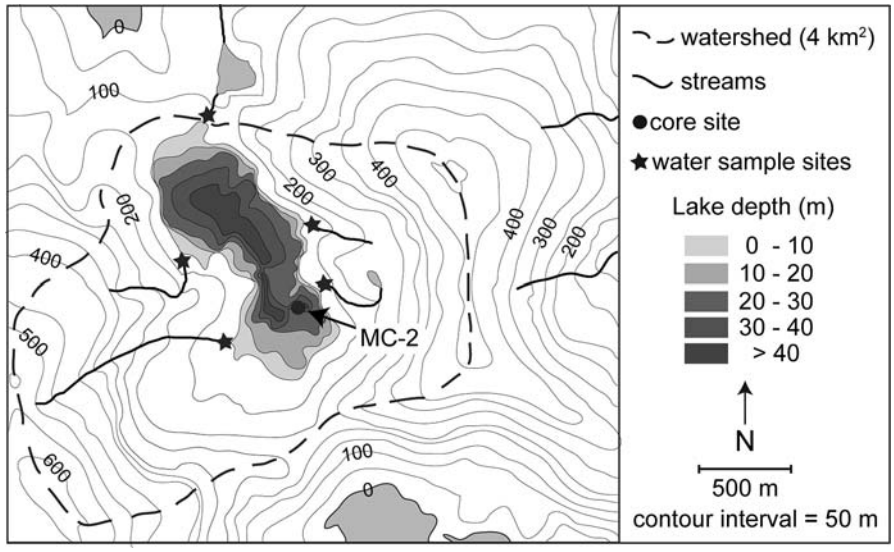

Fig. 4 Mica Lake watershed (dashed line) and bathymetry, with coring (●) and water sampling (★) sites. Map location is shown in Fig. 1

Table 1 Characteristics and surface-water isotope values for surveyed lakes located within 210 km of Mica Lake

Site name/code[a]	Collection date	Latitude (°N)	Longitude (°W)	Elevation (m)	Climate zone[b]	Lake type	Hydrologic setting[c]	$\delta^{18}O$ (‰ VSMOW)	δD (‰ VSMOW)
Robe	Aug-2007	61.085	146.172	9	Maritime	Non-glacial	Open	−15.9	−127
Shrode	Jun-2006	60.652	148.330	24	Maritime	Non-glacial	Open	−14.0	−99
Turner	Jun-2006	60.910	146.627	33	Maritime	Non-glacial	Open	−14.4	−107
Portage	Aug-2007	60.846	148.987	54	Maritime	Glacial	Open	−14.9	−112
Miners	Jun-2006	61.079	147.436	55	Maritime	Glacial	Open	−16.4	−123
Milliard	Jun-2006	60.906	146.578	80	Maritime	Non-glacial	Open	−15.3	−113
Silver	Jun-2006	60.930	146.462	95	Maritime	Glacial	Open	−15.6	−116
“Mica”	Jun-2006	60.692	148.149	100	Maritime	Non-glacial	Open	−12.9	−98
“Mica pond”	Aug-2007	60.694	148.148	103	Maritime	Non-glacial	Closed	−8.6	−63
Bear (Seward Pen)	Aug-2007	60.191	149.358	111	Maritime	Glacial	Open	−14.4	−111
“Cascades”	Jun-2006	60.930	147.869	180	Maritime	Glacial	Open	−14.8	−108
Trail	Aug-2007	60.489	149.368	180	Maritime	Glacial	Open	−17.2	−134
Tern	Aug-2007	60.535	149.545	221	Maritime	Non-glacial	Open	−16.5	−128
Lower Paradise	Jun-2006	60.344	149.074	290	Maritime	Non-glacial	Open	−16.0	−120
Jerome	Aug-2007	60.546	149.570	300	Maritime	Non-glacial	Closed	−15.6	−128
Nellie Juan	Jun-2006	60.248	149.045	350	Maritime	Glacial	Open	−15.9	−117
“Allison”	Jul-2006	61.040	146.349	413	Maritime	Glacial	Open	−16.7	−124
Summit	Aug-2007	60.636	149.504	435	Maritime	Non-glacial	Open	−17.5	−134
Willow	Aug-2007	61.787	145.184	435	Interior	Non-glacial	Closed	−13.3	−129
Long	Aug-2007	61.805	148.234	468	Interior	Non-glacial	Closed	−13.9	−128
“GRS-1”	Aug-2007	62.106	145.471	470	Interior	Non-glacial	Closed	−16.8	−151
“GRS-2”	Aug-2007	61.522	145.226	570	Transitional	Non-glacial	Closed	−15.0	−138
Blueberry	Aug-2007	61.121	145.697	610	Transitional	Non-glacial	Closed	−17.2	−136
Pippin	Aug-2007	61.714	145.161	621	Interior	Non-glacial	Closed	−13.0	−128
Plumbob	Aug-2007	62.107	145.945	624	Interior	Non-glacial	Closed	−14.8	−134
Tolsona	Aug-2007	62.109	146.037	630	Interior	Non-glacial	Open	−13.5	−131
“Ptarmigan”	Aug-2007	61.148	145.723	705	Transitional	Non-glacial	Closed	−18.5	−139
“Lee”	Jul-2006	62.085	146.395	760	Interior	Non-glacial	Closed	−16.1	−143
“Goat”	Jul-006	60.260	149.905	840	Maritime	Non-glacial	Open	−15.9	−123
Greyling	Jul-2006	61.392	145.736	1000	Transitional	Glacial	Open	−20.6	−154
“Eureka”	Aug-2007	61.939	147.168	1010	Interior	Non-glacial	Closed	−15.7	−138
“Hallet”	Jul-2006	61.494	146.238	1160	Transitional	Glacial	Open	−21.5	−160

[a] “ ” indicates informal name

[b] Papineau 2001

[c] Topographic setting closed = no surface outflow

from the littoral zone when logistical constraints limited boat access. The bottles were kept frozen or cool whenever possible.

Hydrogen and oxygen isotope ratios of water samples were measured with a Thermo-Finnigan Deltaplus XL gas isotope-ratio mass spectrometer interfaced to a Thermo-Electron Gasbench II headspace equilibration device at the Colorado Plateau Stable Isotope Laboratory at Northern Arizona University. Analytical precision on internal working standards was ±1‰ for δD and ±0.1‰ for $\delta^{18}O$ and is reported as per mil deviations from the international V-SMOW (Standard Mean Ocean Water) standard.

Sediment core recovery, lithology, and geochronology

In June 2006, percussion cores (7.6 cm diameter up to 3.1 m long) and companion surface gravity cores (6.5 cm diameter up to 0.3 m) were recovered from three sites in Mica Lake. The percussion (MC-2) and surface core (MC-2C) from site 2 (hereafter referred to collectively as 'MC-2') at 58 m depth (Fig. 4), is the longest recovered sediment sequence and is the focus of this study. Coring at this site was presumably halted by the bedrock as evidenced by freshly broken granite fragments lodged in the bottom of the percussion core. Cores were split, photographed, and stored at 4°C. Sediment characteristics and tephra horizons were described and assigned a Munsell soil color. Samples for isotope, biogenic silica (BSi), and organic-matter (OM) analyses, were collected at closer intervals up-core to achieve higher resolution during the last two centuries (0–5 cm, contiguous sampling) and the last 2000 years (10–100 cm, 5 cm spacing), with coarse-sampling for the remainder of the core (100–300 cm, 10 cm spacing). BSi was measured using a wet-alkaline extraction technique (Mortlock and Froelich 1989) and organic matter was measured by loss-on-ignition.

For radiocarbon analyses, 0.5-cm-thick samples were collected at 20 cm spacing, or where vegetation macrofossils were visible, sieved and dried under a laminar-flow hood. AMS ^{14}C analyses were performed at the Keck Carbon Cycle AMS Facility, University of California, Irvine or the Lawrence Livermore National Laboratory, Berkeley, California. ^{210}Pb and ^{137}Cs were measured on two gravity cores, but did not provide interpretable geochronological information (Schiff 2007).

Diatom flora

A preliminary diatom stratigraphy was generated from the Mica Lake sequence to assess the extent that $\delta^{18}O_{diatom}$ correlates with diatom floristic composition. Diatoms were examined every 20 cm (i.e. 15 samples), thus capturing each phase of Holocene lake development, albeit at coarse resolution. Diatom samples (200 mg dry sediment) were processed with successive digestions in 10% and 30% H_2O_2. Digested slurries were diluted and strewn onto coverslips, dried at room temperature, and mounted to slides with Naphrax® medium. Taxonomic resolution was limited to genus level (Round et al. 1990) because this investigation aimed to assess only major shifts in the diatom community.

Relationships between diatom assemblage composition and sediment geochemical variables were evaluated objectively using principal components analysis (PCA), an indirect linear ordination method (ter Braak and Prentice 1988). PCA was applied to a correlation matrix including the relative frequencies of the dominant diatom genera observed (*Achnanthes*, *Aulacoseira*, *Encyonema*, *Eunotia*, *Fragilaria sensu lato*, *Frustulia*, *Navicula*, and *Pinnularia*) as well as corresponding OM, BSi, and $\delta^{18}O_{diatom}$ values for the 15 core depths under consideration. Pre-screening of the data indicated very short first axis gradients (i.e. 0.49 standard deviation units), attesting to the suitability of linear ordination approaches. The ordination was conducted using CANOCO software running under Windows (ter Braak and Smilauer 1998).

Diatom isolation and analyses

Diatoms from 46, 0.5-cm-thick samples were isolated and analyzed for their oxygen isotope composition ($\delta^{18}O_{diatom}$). Pure diatoms must be isolated because other lake sediment components (e.g. tephra, mineral grains, organic matter) contain oxygen that is liberated during fluorination of the sample for mass spectrometer analyses (Leng and Barker 2006). A three-stage protocol, involving chemical digestion, wet sieving, and heavy-liquid separation, was adapted from Morley et al. (2004). Diatom extracts were screened for purity using a high-powered microscope, and a scanning electron microscope (SEM) was used to further confirm the purity of selected intervals (Fig. 5). The 10- to 50-μm size fraction was the purest.

The silica of diatom frustules includes an outer hydrous layer and a denser inner layer. Oxygen in the inner layer is isotopically homogenous, but the outer layer freely exchanges with the ambient water after formation (Juillet 1980). Therefore, diatom silica must be dehydrated prior to mass spectrometry analyses to obtain an isotope value representative of the lake water at the time of frustule formation. Numerous methods have been used to remove the outer hydrous layer, including vacuum dehydration,

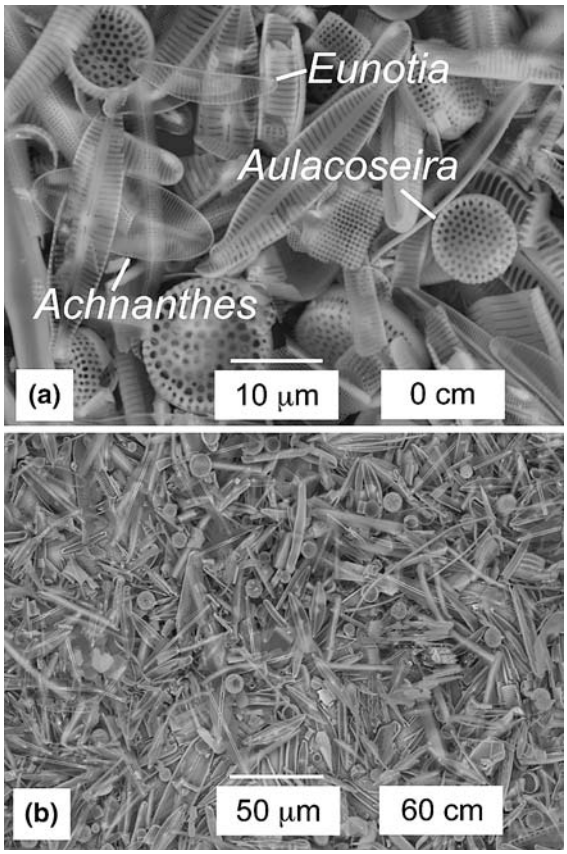

Fig. 5 Backscattered electron microscope image of purified diatom samples from (**a**) 0 cm and (**b**) 60 cm depth in core MC-2

isotope exchange, and stepwise fluorination (Leng and Barker 2006). Recently, a stepwise fluorination technique was designed that uses a CO_2 laser-ablation system, coupled to a mass spectrometer (Dodd et al. 2007). This study is the first to employ the new method to analyze lacustrine diatoms. The new technique is rapid and requires only 1–2 mg of pure diatoms, which is less than the 5 mg typically used for stepwise fluorination techniques. It differs from previous techniques in that water is removed by low-temperature fluorination with F_2 gas, followed by reaction with BrF_5 at high temperatures. $\delta^{18}O_{diatom}$ analyses were made at the University of New Mexico, Albuquerque. The in-house quartz standard, Gee Whiz ($\delta^{18}O = +12.65 \pm 0.15‰$), and an in-house diatomite monitor of reproducibility, SR2-1B ($\delta^{18}O = +32.3 \pm 0.2‰$), were analyzed routinely with each batch of 10–18 samples. Gee Whiz has been calibrated to the international NBS quartz standard ($\delta^{18}O = +9.6‰$) at the University of New Mexico. Ten samples were randomly selected from the MC-2 sequence and prepared and analyzed in duplicate. The $\delta^{18}O$ values of these repeat analyses ranged from +24.9‰ to +29.4‰, and the reproducibility averaged +0.2‰, which is the uncertainty assigned to diatom samples analyzed over the course of this study. Results are presented in conventional δ notation relative to the V-SMOW standard.

Results[1]

Regional hydrogen and oxygen isotope values of lake water

δW values in water of 72 samples collected from south Alaska during the 2006 and 2007 summers range from −22.6 to −5.9‰, and −176 to −38‰ for $\delta^{18}O$ and δD, respectively (Fig. 6). Data from each of the three climate zones define local water lines (Fig. 6b-c). Broadly, δW values trend from high to low, then back to high values along the south-to-north moisture pathway. In Prince William Sound, $\delta^{18}O$ and δD define the local meteoric water line (LMWL), which is parallel to the global meteoric water line (GMWL) (Fig. 6b). In the transitional climate zone, $\delta^{18}O$ and δD are generally lower and the data define local evaporation lines with slopes ($\sim$6), less than the LMWL and GMWL (8) (Fig. 6c). The lower δW values reflect the cooler temperatures at the higher sites sampled in this climatic zone, and rain-out of moisture that is transported north over the Chugach Mountains. The lower slope is due to enrichment of surface water in ^{18}O, relative to D, caused by evaporation (Gat 1981), and the data therefore depart from the GMWL. Similarly, water from the interior sites has relatively high $\delta^{18}O$ values and a slope ($\sim$6) parallel to the local evaporation lines (Fig. 6d). High $\delta^{18}O$ and relatively low δD values at interior sites are due to evaporation.

At Mica Lake, surface, bottom, inflow, and outflow water ($n = 15$) have a narrow range of $\delta^{18}O$ values (−12.7 to −13.3‰). This observation,

[1] All $\delta^{18}O_{diatom}$, BSi, and OM data presented in this study are available on-line at the World Data Center for Paleoclimatology (ftp://ftp.ncdc.noaa.gov/pub/data/paleo/paleolimnology/northamerica/usa/alaska/mica2008.txt).

combined with similarity to the GMWL, suggests that the lake is well mixed and evaporation does not greatly alter its isotopic values.

Core chronology

Sixteen ^{14}C ages were calibrated to calendar years using the IntCal04 calibration curve (Reimer et al. 2004) and CALIB (v 5.0.2; Stuiver and Reimer 1993). We used the median probability age output by CALIB as the single best estimate of the central tendency of the calibrated age (Telford et al. 2004), and report all ages in reference to calendar year 1950 AD (cal BP, or thousands of calendar years, ka). Thirteen calibrated ages on terrestrial and aquatic macrofossils (Table 2) and the age of the sediment surface (0 cm = −56 cal BP) were combined to construct a depth-age model for core MC-2 (Fig. 7). Three ages were not included in the age model because they were on terrestrial vegetation that yielded ages older than underlying ages and were inferred to be substantially older than the surrounding sediment, or because they were from a sand-rich layer, interpreted to be an avalanche deposit (Schiff 2007). Adjusted depth below lake floor (blf) for each dated layer was calculated by removing the thickness of tephra layers and avalanche deposits. A spline fit was constructed using formulations from Heegaard et al. (2005) and the statistical software R (http://cran.r-project.org; last accessed 20 December 2007), as described by Schiff et al. (2008). The model takes into account both the uncertainty in the calibrated ages as well as the uncertainty in how well the age represents a particular core level. In addition to an age-depth model, the procedure generates the 95% confidence intervals. A k-value of 7 was selected for MC-2 because it is the lowest value that contains all but one of the 2σ ranges of the calibrated ages, and has relatively low model residuals, calculated as the difference between the calibrated and estimated age of each dated level. The conflicting ^{210}Pb and ^{137}Cs results from two gravity cores (Schiff 2007) suggest

Table 2 Radiocarbon and calibrated ages from core MC-2

Adjusted depth blf (cm)[a]	^{14}C age (year BP)	Calibrated age (cal year)[b]	Dated material[c]	Lab ID
4.25	285 ± 15	380 ± 60	Wood	29509[d]
24.50[f]	1350 ± 15	1290 ± 5	Hemlock needles	29510[d]
25.25[f]	1180 ± 20	1110 ± 55	Hemlock needles	134202[e]
24.00[f]	1500 ± 35	1380 ± 35	Mixed macrofossils	134203[e]
26.00	1200 ± 40	1125 ± 55	Hemlock needles	33147[d]
36.00	1390 ± 20	1300 ± 10	Hemlock needles	29511[d]
54.25	1565 ± 15	1470 ± 50	Mixed macrofossils	134204[e]
55.00	1655 ± 40	1555 ± 85	Hemlock needles	33148[d]
65.00	2040 ± 60	2010 ± 90	Aquatic moss	134205[e]
74.75	2390 ± 70	2460 ± 170	Mixed macrofossils	134206[e]
85.00	2790 ± 70	2900 ± 85	Aquatic moss	134207[e]
133.50	3580 ± 15	3880 ± 25	Bark	29512[d]
149.75	4135 ± 20	4680 ± 110	Hemlock needles	33149[d]
177.50[f]	5975 ± 25	6815 ± 50	Bark	29513[d]
188.25	5135 ± 20	5910 ± 10	Aquatic moss	33150[d]
276.75	8500 ± 60	9500 ± 30	Mixed macrofossils	34298[d]

[a] Centered sample depth; samples 0.25–0.50 cm thick

[b] Median probability ± one-half of 1s age range from CALIB v.5.0.2 (Stuiver and Reimer 1993)

[c] Mixed macrofossils include various proportions of aquatic moss, Hemlock needles, wood, and leaf fragments

[d] Lawrence Livermore National Laboratory, Center for Accelerator Mass Spectrometry (CAMS)

[e] Keck Carbon Cycle AMS Facility, University of California Irvine (UCIAMS)

[f] Excluded from age model

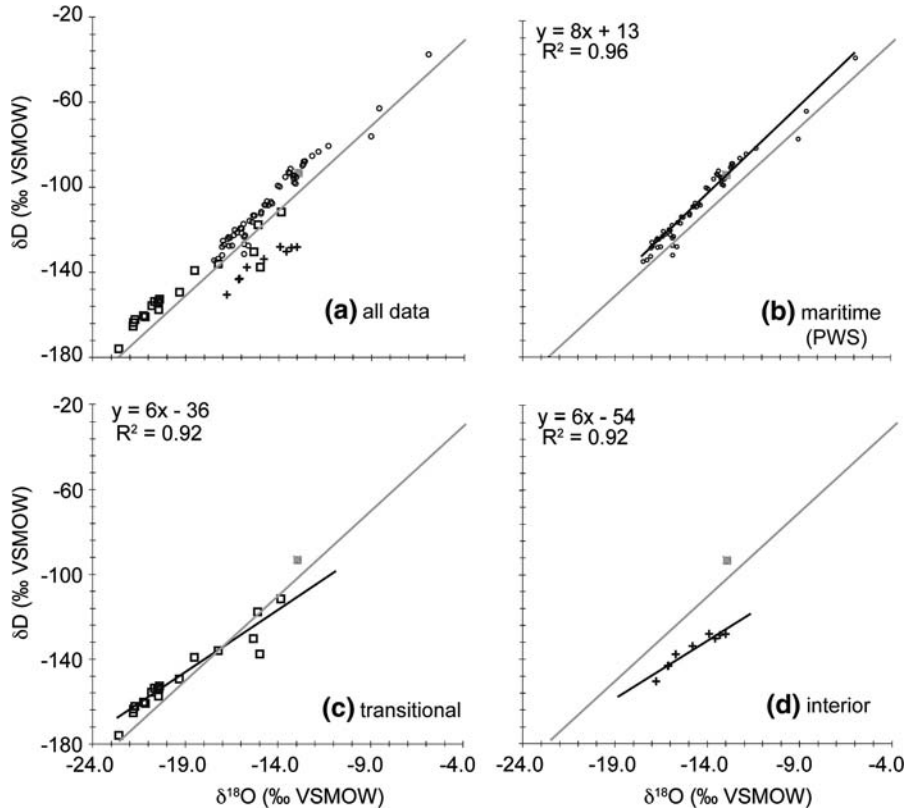

Fig. 6 Oxygen and hydrogen isotope values for water samples from south Alaska lakes, 2006 and 2007. **a** Different symbols indicate different climate regimes, **b** Prince William Sound (PWS) (□), **c** transitional (◯), and **d** interior samples (✚). Gray line is the global meteoric water line [GMWL; $\delta D = 8\ \delta^{18}O + 10$ (Dansgaard 1964)] and gray square is Mica Lake surface water. The slope and distance from the GMWL of the least-squares regression for each region indicates evaporative effects. Note that the Prince William Sound line is parallel with the GMWL

that the youngest sediment may be disturbed. As such, the age of these sediments is less certain.

Using this age model, the age of the base of the core is extrapolated to 9910 cal BP. The basal age provides a minimum age of deglaciation at Mica Lake. The average sedimentation rate is 0.30 mm year^{-1}. Therefore, each 0.5 cm sample represents ~15 year of sedimentation. The average age uncertainty based on the 95% confidence interval is ±112 year.

Core lithostratigraphy and diatom flora

Core MC-2 contains massive gyttja, sand layers, and tephra deposits (Fig. 8). The average organic matter and biogenic silica content of the massive gyttja units is 19% and 5%, respectively (Schiff 2007). The coarse-grained sand layers contain abundant terrestrial macrofossils and are interpreted as avalanche deposits, an interpretation that is consistent with the steep-sided basin, especially near core site 2 (Fig. 4). Six tephra deposits were located based on high magnetic susceptibility values and visual inspection (Fig. 7, inset table).

Diatom assemblages from Mica Lake are similar to low-alkalinity sites elsewhere in Alaska (Hein 1990; Gregory-Eaves et al. 1999), with a preponderance of circumneutral to acidophilic forms belonging to the genera *Achnanthes*, *Aulacoseira*, and *Eunotia*. Stratigraphically, the largest assemblage changes occur during the last millennium, when frequencies of *Achnanthes* decline abruptly, and proportions of larger benthic genera (e.g. *Frustulia* and *Pinnularia*) increase. Between 9600 and 1000 cal BP, diatom assemblages are characterized by progressive declines in the representation of *Aulacoseira*, and increases of *Eunotia* and a number of benthic genera.

These stratigraphic changes are captured efficiently by the biplot of the first two PCA axes extracted from the combined diatom, BSi and OM data (Fig. 9). Collectively, these PCA axes account for 57.1% of variance in the dataset ($\lambda_1 = 0.338$; $\lambda_2 = 0.233$); lower-order axes are not considered in this study. The time-trajectory of PCA sample scores along these axes differentiates three distinct stratigraphic zones: 300–140 cm (9600–4000 cal BP);

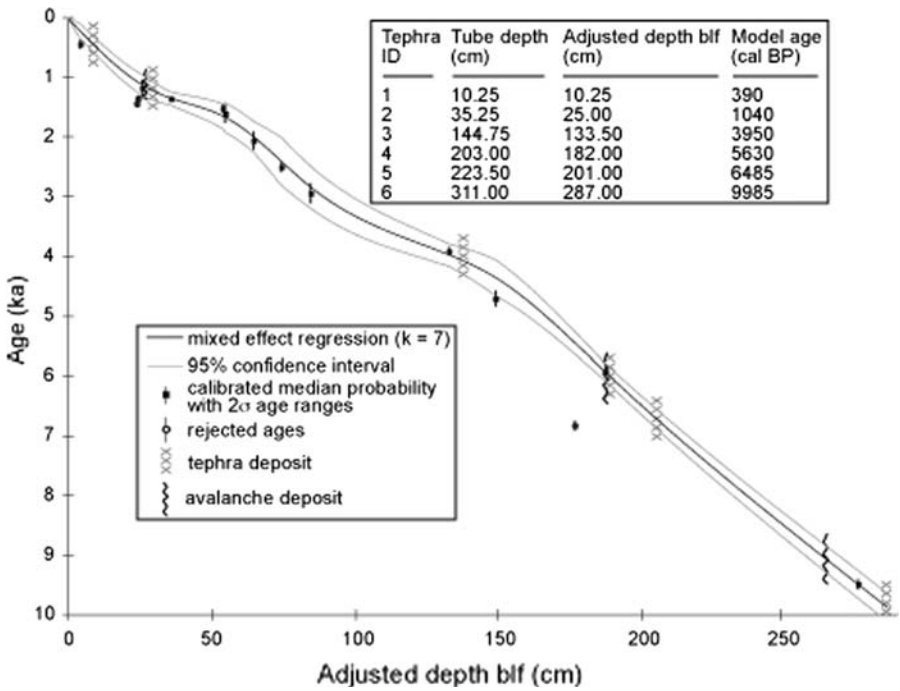

Fig. 7 Spline fit (Heegaard et al. 2005) through 13 AMS ^{14}C ages (see text for details) and the age of the surface sediment (2006). The depth of each dated level was determined after subtracting the cumulative thickness of tephra and avalanche deposits. ^{14}C data are listed in Table 2

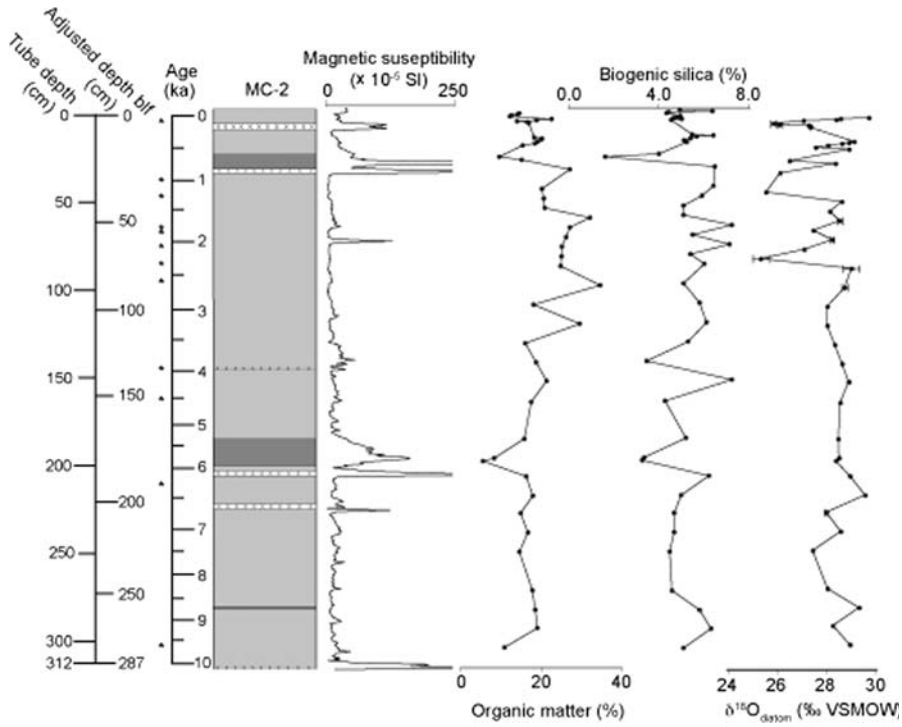

Fig. 8 Summary of core MC-2 stratigraphy. Adjusted depth below lake floor (blf) was calculated by subtracting the thickness of overlying tephra and avalanche deposits (total of 24.5 cm) from tube depth. * = depth of ^{14}C ages (Table 2). Light gray = massive gyttja, dark gray = sand layer, and X = tephra layer (Fig. 7 inset table). Further description of lithologic units is provided by Schiff (2007). Error bars for $\delta^{18}O_{diatom}$ based on duplicate or triplicate analyses

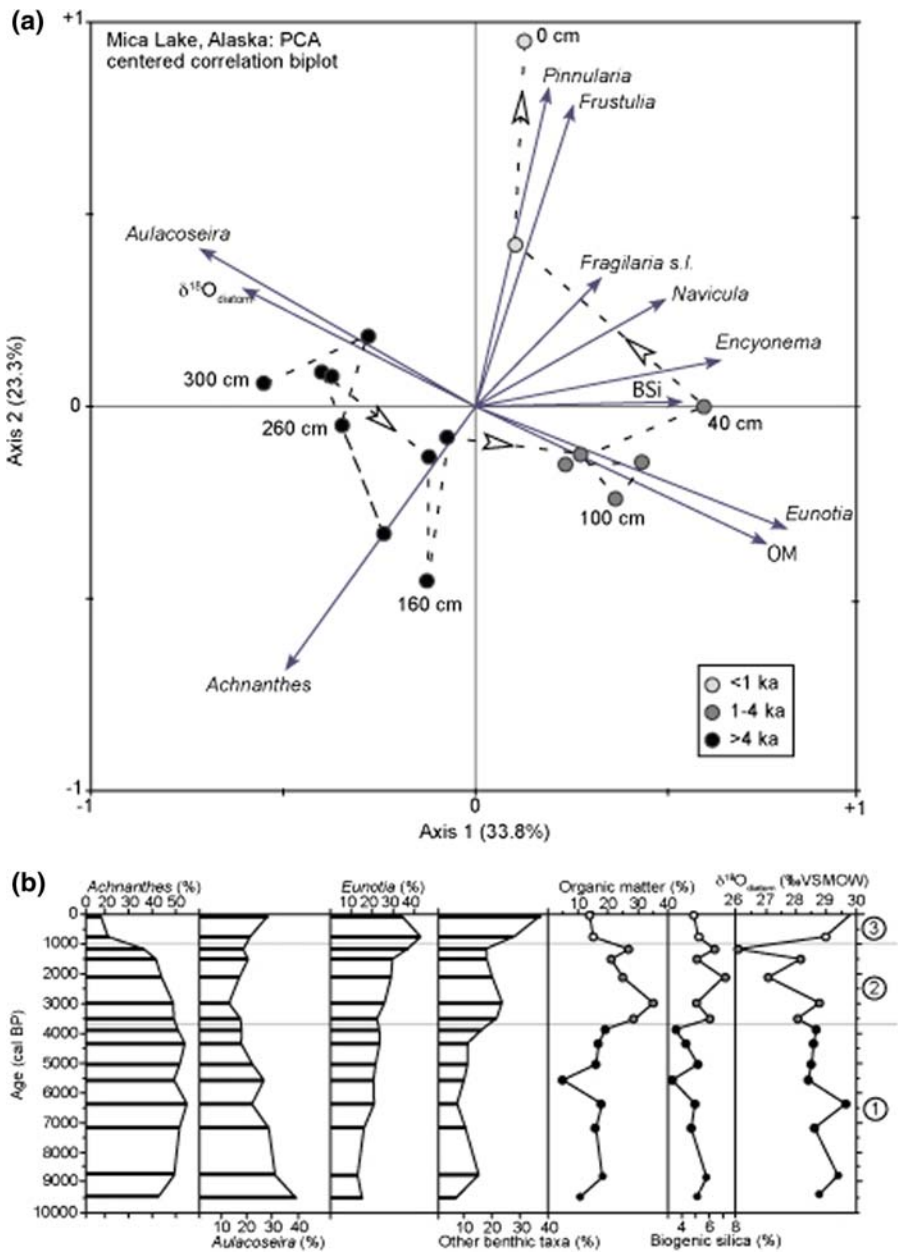

Fig. 9 **a** Principal component analysis of Mica Lake $\delta^{18}O_{diatom}$, biogenic silica (BSi), organic matter (OM), and dominant diatom genera. **b** Stratigraphic changes of the most dominant diatom genera at Mica Lake compared with $\delta^{18}O_{diatom}$, BSi, and OM. Three distinct stratigraphic zones were identified by the time-trajectory PCA: 300–140 cm (9600–4000 cal BP); 120–40 cm (4000–1000 cal BP); and 40–0 cm (1000 cal BP to present)

120–40 cm (4000–1000 cal BP); and 40–0 cm (1000 cal BP to present).

Oxygen isotope values of diatoms from Mica Lake

Forty-six downcore $\delta^{18}O_{diatom}$ values from MC-2 range between +25.2 and +29.8‰ (Table 3; Fig. 10a). Prior to 2.6 ka, the values range by only +2.2‰. At 2.6 ka, $\delta^{18}O_{diatom}$ exhibits a strong shift to values that vary as much as +4.6‰. The youngest sample, which probably represents the last ~15 year, contains the highest $\delta^{18}O_{diatom}$ value at +29.8‰. Within the analytical precision of the laser-extraction technique (±0.2‰), only one other sample, at 6.4 ka, has a comparable value. Mica Lake water, collected during the summers of 2006 and 2007, has an average ($n = 6$) $\delta^{18}O$ value of −13.0‰; the measured

Table 3 $\delta^{18}O_{diatom}$ data from core MC-2

Adjusted depth blf (cm)	Age (cal BP)[a]	$\delta^{18}O_{diatom}$ (‰ VSMOW)			
		Run 1	Run 2	Average	SD
0.25	−44			29.8	
0.75	−18			28.6	
1.25	7			28.4	
1.75	32			27.0	
3.25	107	25.9	25.7	25.8	0.1
3.75	132	26.2	25.9	26.0	0.2
4.25	156			27.3	
4.75	181			27.4	
5.25	206			27.3	
12.75	563			29.2	
13.25	586			29.0	
13.75	609			28.7	
14.75	652			28.1	
15.75	696			27.6	
16.75	738			29.0	
22.75	967			26.5	
24.25	1017			28.4	
29.25	1159			26.1	
39.25	1350			25.5	
44.25	1422			28.7	
49.25	1500	28.2	28.2	28.2	0.0
54.25	1601	28.7	28.5	28.6	0.1
59.25	1740			27.5	
64.25	1916	28.2	28.3	28.3	0.1
69.25	2120			27.1	
74.25	2340	25.6	24.9	25.2	0.5
79.25	2561	29.4	28.7	29.1	0.5
89.25	2955	28.9	28.7	28.8	0.2
99.25	3257			28.0	
109.25	3492			28.0	
119.25	3687			28.4	
129.25	3869			28.7	
138.75	4055	29.0	28.9	29.0	0.0
149.75	4330			28.6	
168.75	5036			28.5	
178.75	5482			28.5	
180.25	5551			28.4	
188.25	5917			29.0	
198.25	6364			29.6	
207.25	6753	28.0	28.0	28.0	0.0
217.25	7173			28.6	
227.25	7582			27.4	
247.25	8373			28.1	
257.25	8759			29.4	
266.75	9123			28.3	
276.75	9504			29.0	

[a] Ages based on model shown in Fig. 7

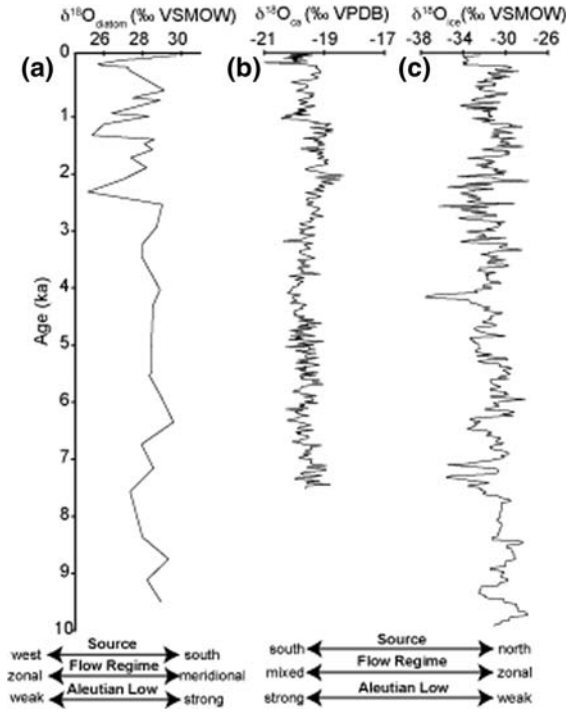

Fig. 10 Oxygen isotope records from (**a**) Mica Lake diatoms compared to other North Pacific $\delta^{18}O$ records from (**b**) Jellybean Lake carbonate (Anderson et al. 2005) and (**c**) Mt. Logan ice cores. The inferred influences of climatic controls discussed in the text are indicated. The climatic interpretations suggested from model simulations by Fisher et al. (2004) explain the variability at Jellybean Lake and Mt. Logan. Age of $\delta^{18}O_{diatom}$ from Mica Lake based on age model in Fig. 7

isotopic partitioning between modern water and diatoms is +42.8‰. Similar differences between isotope values measured in water and diatoms from surface sediment have been measured at four other lakes in south-central Alaska (Schiff 2007). Even higher partitioning values (+44.3‰) have been reported from marine diatoms (Juillet-Leclerc and Labeyrie 1987). However, cultured diatoms exhibit far lesser degrees of oxygen isotopic enrichment

relative to ambient water (Brandriss et al. 1998), implying that additional isotopic discrimination processes exist in natural environments that are not captured in culturing experiments.

Controls on $\delta^{18}O_{diatom}$ in southern Alaska

Non-climatic controls

Diagenetic effects have been reported in studies that compare the oxygen isotope ratios in diatoms collected in traps versus those extracted from sediment (e.g. Moschen et al. 2006). These studies found a slow-acting maturation of diatoms that led to enrichment of values after deposition. The authors attribute the enrichment to silica dissolution and dehydroxylation and suggest that $\delta^{18}O_{diatom}$ records with long-term trends of enrichment with age should consider diagenetic effects as a leading explanation. Backscattered electron microscope images show no obvious dissolution of modern (Fig. 5a; 0 cm) or mid-Holocene (Fig. 5b; 60 cm) diatom frustules from MC-2. This observation, combined with the lack of a long-term trend in the MC-2 record suggests that diagenetic effects are absent or undetectable at Mica Lake.

Diatom habitat and taxonomic (vital) effects might influence $\delta^{18}O_{diatom}$ values. Because diatoms live in both benthic and planktonic settings, they experience different temperatures through most of the year. Benthic and planktonic diatoms formed at the same time could have different isotope values, particularly if the lake water $\delta^{18}O$ value or temperature were different between habitats. At Mica Lake, however, surface and bottom water during June 2006 and August 2007 had nearly identical $\delta^{18}O$ values, suggesting the lake is well mixed during the late spring and summer.

In Mica Lake, the three zones recognized in the diatom assemblages are entirely coherent with the $\delta^{18}O_{diatom}$ record, suggesting that the same climatic factors that regulated lake water and diatom $\delta^{18}O$ also influenced the composition of diatom assemblage. Of the diatom genera encountered, *Aulacoseira* and *Eunotia* are the most closely associated with the loading vector of $\delta^{18}O_{diatom}$ on the first 2 PCA axes, in positive and negative associations, respectively (Fig. 9a). These results are consistent with the expansion of planktonic and tychoplanktonic genera such as *Aulacoseira* under relatively warm conditions with prolonged open-water seasons (Smol et al. 2005), as well as with increased representations of acidophilic diatoms (e.g. *Eunotia* spp.) during cold intervals (Wolfe 2002).

There is, however, no evidence that diatom assemblage composition exerts a first-order control over $\delta^{18}O_{diatom}$ values. Diatom genera other than *Aulacoseria* and *Eunotia* appear unrelated to the vector of $\delta^{18}O_{diatom}$ in PCA, with several genera being orthogonal to this gradient (*Achnanthes*, *Frustulia*, and *Pinnularia*). The stratigraphy of summed benthic diatoms, excluding *Achnanthes* and *Eunotia* (Fig. 9b), confirms this point: these taxa increase initially as $\delta^{18}O_{diatom}$ values decline after 4.0 ka, but continue to expand during the subsequent recovery of $\delta^{18}O_{diatom}$ in the last millennium.

We therefore surmise that the stratigraphic trends of *Eunotia* and *Aulacoseira* are predictable ecological responses to the climate shifts suggested by the Mica Lake $\delta^{18}O_{diatom}$ record, rather than driving the isotopic signal through species-specific differences in $^{18}O/^{16}O$ fractionation. These results are compatible with experimental studies that revealed scant evidence for metabolic differences in oxygen isotope fractionation among diatom genera (Brandriss et al. 1998) although Swann et al. (2008) found evidence of a vital effect in marine diatoms.

Climatic controls

The inability of water temperature—diatom fractionation and non-climatic factors to fully explain the large variability of Holocene $\delta^{18}O_{diatom}$ values suggests that the $\delta^{18}O$ value of Mica Lake water has varied over the last 9600 cal BP. The two primary controls on lake water $\delta^{18}O$ are the P/E balance and the $\delta^{18}O$ of the inflow, both of which vary with climate.

P/E balance

The P/E balance strongly influences δW of lakes (Gat 1981). δW data from the lakes surveyed in this study exemplify these influences: interior lakes, receiving low precipitation are hydrologically closed (Table 1), and evaporation at these sites causes enrichment in D and ^{18}O, which shift values off the

GMWL (Fig. 6d) (Gat 1981). In contrast, lakes in the Prince William Sound receive an average of about 3 m of precipitation a year, and δW is influenced only slightly by evaporation. At Mica Lake, surface and bottom waters collected in June 2006 and August 2007 suggest a small progressive isotopic enrichment of surface water from summer evaporation: δ^{18}O values of bottom water are nearly identical between summers (−13.2 and −13.4‰), whereas the surface water from August 2007 is +0.5‰ enriched relative to June 2006. The enrichment is small when compared with the late Holocene +4.6‰ range of $\delta^{18}O_{diatom}$ at Mica Lake, and might be irrelevant if diatom blooms always occur during the late spring, prior to progressive evaporation through the summer months. Furthermore, surface water inflow into Mica Lake collected during the summer is indistinguishable from Mica Lake surface water.

Using a range of precipitation rates from 3 to 7 m year^{-1}, which encompasses the observed rate at Whittier during the last 25 year (average = 5.5 m year^{-1}), and assuming that evapotranspiration is less than 0.5 m year^{-1}, which is typical for south Alaska (Newman and Branton 1972), the lake water residence time is <5 year at Mica Lake. Lakes with such low residence time are relatively unaffected by evaporation (Leng and Marshall 2004).

Taken together, the high precipitation input, short water residence time, nearly homogenous δW at Mica Lake, and overlap with the local meteoric water line (Fig. 6), suggest that the modern δW is not affected strongly by evaporation, and instead is controlled largely by δP. This conclusion is supported by the long-term $\delta^{18}O_{diatom}$ record from Mica Lake. The δW of lakes is typically elevated and variable when evaporation exerts a strong control, whereas δW is generally low and relatively constant during wet periods (Leng and Marshall 2004). At first glance, therefore, the increased late Holocene variability in $\delta^{18}O_{diatom}$ at Mica Lake (2.6 ka to modern; Fig. 10a) could reflect increased evaporation. On the other hand, the shift to lower $\delta^{18}O_{diatom}$ values following 2.6 ka and the coincidence with the increased variability is inconsistent with the hypothesis of increased evaporation. We cannot entirely rule out evaporative effects during the early and middle Holocene, but the most recent $\delta^{18}O_{diatom}$ value is the highest (+29.8‰), so any changes in P/E are likely masked by stronger controls. Isotope analyses of diatom samples containing other sediment components (e.g. tephra, mineral grains) (Brewer et al. 2008) would yield lower values, but our SEM screening did not reveal contamination.

Seasonality of precipitation

Seasonal differences in δP could affect δW if the seasonality of precipitation has varied. The relatively sparse IAEA-GNIP data available for the North Pacific region (Fig. 1 inset) provide some insight into the seasonal range of δP in south Alaska. The maritime climate at Mica Lake is most similar to the Adak IAEA-GNIP station, located 2000 km to the west (Fig. 1 inset). IAEA-GNIP data collected between 1962 and 1973 record mean summer (JJA) temperature at Adak that is +9°C higher than winter (DJF) temperatures, whereas mean δ^{18}O is +0.4‰ higher in summer compared to winter. Applying the ^{18}O—air temperature fractionation from the IAEA-GNIP global dataset (+0.65‰ °C^{-1}; Rozanski et al. 1993) to the +9°C seasonal temperature range implies a range of +5.9‰ between summer and winter, which is an order of magnitude greater than what is recorded. The amount of precipitation, on the other hand, is more strongly correlated to δ^{18}O values in the Adak dataset: monthly δ^{18}O is inversely related to the amount of precipitation ($r = -0.50$, $p < 0.1$). If the Adak data are representative of conditions at Mica Lake, higher $\delta^{18}O_{diatom}$ might represent decreased precipitation, but is likely insensitive to changes in seasonality of precipitation because the seasonal range of δ^{18}O is low. The general similarity between climate at Adak and the Prince William Sound is not necessarily a good indication that δP from the two areas should correlate, however. To further investigate the "amount effect" in the North Pacific, a common phenomenon at low latitudes, year-long collections are needed.

Air temperature

The global relationship between δP and temperature (i.e. 'Dansgaard effect') ranges between ~+0.2 and +0.9‰ °C^{-1} (Rozanski et al. 1993). Applying these slopes to the range in $\delta^{18}O_{diatom}$ at Mica Lake (~+4.6‰) suggests a shift of +5 to +23°C during the late Holocene. The upper estimate is not plausible, whereas the lower estimate is similar to the DJF temperature range observed between the ten strongest

and weakest Aleutian Low years at climate stations in south Alaska (Fig. 2b). The paucity of IAEA-GNIP data from the region precludes an accurate assessment of the influence of air temperature on δP.

Changes in storm trajectories

The increase in $\delta^{18}O_{diatom}$ values between the mid-19th century to present (+4.0‰) from MC-2 might be explained more reasonably by changes in storm trajectories. Specifically, moisture from the west and north Pacific, delivered by zonal (west-to-east trajectory) flow, is longer-traveled and likely more depleted in heavy isotopes than moisture delivered by meridional (south-to-north trajectory) flow, which for south Alaska is likely from the Gulf of Alaska (Cayan and Peterson 1989). Moisture from zonal flow crosses southwest Alaska and is susceptible to rain-out as it passes over land, whereas moisture from meridional flow travels over the Gulf of Alaska and generates less rain-out. Without more complete collections of precipitation, we cannot provide a quantitative estimate of the change in δP from different storm trajectories. Nevertheless, changing storm trajectory has been observed to cause large variations in δP (e.g. Lawrence et al. 1982).

Winter storm trajectories are closely linked to the strength and position of the Aleutian Low. During strong Aleutian Low years, most storms that intersect south Alaska have a south-to-north trajectory and the moisture contribution from the Gulf of Alaska is likely large (Fig. 2a). During weak Aleutian Low years, storm origins are more often divided into two loci and the south-to-north storm trajectory is less prominent (Fig. 2a). The weaker meridional flow might allow zonal flow to deliver moisture from along a west-to-east storm trajectory to reach south Alaska. Furthermore, surface air temperature in south Alaska during strong Aleutian Low years is about +5°C warmer than weak Aleutian Low years (Fig. 2b), which supports the hypothesis of greater meridional flow. As previously mentioned, the increased temperature would likely cause increased $\delta^{18}O$ and the seasonal variability of $\delta^{18}O$ at the coastal IAEA-GNIP site is low (+0.4‰), so greater winter precipitation during strong Aleutian Low years would not reduce greatly the annual $\delta^{18}O$ average.

On the basis of this interpretation, the Mica Lake $\delta^{18}O_{diatom}$ record suggests that the moisture delivery to south Alaska has shifted between zonal and meridional flow during the last 2.6 ka (Fig. 10a). Low $\delta^{18}O_{diatom}$ values reflect zonal flow. Before 2.6 ka, the record is relatively stable and has generally high $\delta^{18}O_{diatom}$ values, suggesting enhanced meridional flow.

Discussion

North Pacific paleoclimate records from lake sediments (e.g. Hu et al. 2001; McKay 2007), glacier advances (e.g. Wiles et al. 2008), and tree rings (e.g. Wilson et al. 2007) document strong climate variability during the late Holocene. Most records point to some influence from the variability of the Aleutian Low, usually building on the relationship between changes during the 20th century and proxy data (e.g. Anderson et al. 2005; McKay 2007). For example, in a summary of pollen records from northwest North America, Spooner et al. (2003) showed that the occurrence of far-traveled pollen increased at multiple sites across northwest British Columbia from ~3 ka to present; the likely mechanism is thought to be a long-lasting phase of strong Aleutian Low because coastal pollen is more frequently carried inland during strong Aleutian Low. Accumulation rates at Mt. Logan between 1948 and 1987 are correlated with warm phases of ENSO, which correspond to increased south-to-north storm trajectories in the North Pacific (Moore et al. 2003). Similar to these Pacific paleoclimate records, the large variability of $\delta^{18}O_{diatom}$ values at Mica Lake suggests pronounced shifts in wintertime circulation.

Comparisons with other paleorecords of δP in the North Pacific

Paleorecords of δP from the North Pacific region are few, but a connection to large-scale atmospheric circulation is beginning to emerge. Oxygen isotope ratios of authigenic carbonate ($\delta^{18}O_{ca}$) from Holocene sediment of Jellybean Lake, Yukon Territory (Fig. 1 inset) range by ~2‰ (Fig. 10b), which is too large to be explained by changing water temperatures (Anderson et al. 2005). Rather, $\delta^{18}O_{ca}$ values at Jellybean Lake are interpreted as a proxy for the intensity and position of the Aleutian Low. The data from Jellybean Lake suggest greater isotopic

distillation of air masses during times of strong Aleutian Low because meridional flow brings stronger leeward winds to southwestern Yukon Territory. Meridional flow delivers precipitation with high $\delta^{18}O$ values at Mica Lake, but low $\delta^{18}O$ values at Jellybean Lake because the coastal setting of Mica Lake limits rain-out under meridional flow, while rain-out is enhanced at the interior setting of Jellybean Lake.

Oxygen isotope ratios from an ice core ($\delta^{18}O_{ice}$) from the Mt. Logan summit (Fig. 1 inset) do not correlate with instrumental or paleotemperature data from the region (Holdsworth et al. 1992), although annual precipitation totals correlate with North Pacific climate indices (Moore et al. 2002). The $\delta^{18}O_{ice}$ values from Eclipse Icefield (Fig. 1 inset) are correlated significantly with northwestern North America temperature, but the correlation explains only between 5 and 10% of the variability (Wake et al. 2002). These results suggest site temperature is not the primary control of δP in the North Pacific.

Using an isotope model simulation, Fisher et al. (2004) suggest that isotope variability at Mt. Logan and Jellybean Lake can be explained by shifting moisture source. More specifically, two atmospheric flow regimes are prescribed for the model and provide a mechanism to explain changes in δP: under the mixed (meridional) flow regime, the moisture source includes low latitudes, whereas the zonal flow regime derives moisture strictly from the high latitudes of the North Pacific. The model predicts vertically stratified differences in δP between each flow regime. The difference between mixed and zonal regimes [$\delta^{18}O$ (zonal) $-$ $\delta^{18}O$ (mixed)] above 1 km altitude is positive, and negative below 1 km. High-elevation sites receive relatively light δP under mixed flow, while low-elevation sites receive heavy δP. The site response under the two different flow regimes is expected to be opposite at Mica Lake (median catchment elevation = 364 m asl) compared to Jellybean Lake (effective catchment elevation = 1650 m asl) and Mt. Logan (5340 m asl).

In general, the range of $\delta^{18}O$ values during early and mid-Holocene at Mica and Jellybean Lakes is lower than during the late Holocene (Fig. 10a and b). In contrast, Mt. Logan $\delta^{18}O_{ice}$ values do not show a late Holocene shift to more variable values (Fig. 10c). The inverse relationship between $\delta^{18}O$ values at Mica Lake versus Jellybean Lake and Mt. Logan is not strongly evident, and depends on the quality of the geochronology. However, the shift to more variable and lower $\delta^{18}O_{diatom}$ values at Mica Lake at 2.6 ka is coincident with generally increasing $\delta^{18}O$ values at both Jellybean Lake and Mt. Logan, suggesting that moisture delivery shifted from meridional to zonal flow at all sites.

The Little Ice Age

The most recent shift to lower $\delta^{18}O_{diatom}$ values at Mica Lake coincides with the Little Ice Age, a time of widespread cooling. The Little Ice Age is well documented in the North Pacific region. Most glaciers in south Alaska reached their Holocene maxima during the Little Ice Age (Wiles et al. 2008), suggesting that either summer temperature reached its minimum, or that winter precipitation was at its maximum, or both. Studies of glacier equilibrium-line altitudes find that lower summer temperatures and lower winter precipitation occurred during the Little Ice Age; the latter suggest a weaker Aleutian Low (Daigle and Kaufman 2008; McKay 2007). These proxy records compare well with the low $\delta^{18}O_{diatom}$ values at Mica Lake of +26.0 and +25.8‰ at 1820 and 1845 AD, respectively, which is interpreted as a period of weak Aleutian Low, when south Alaska received relatively more moisture from zonal flow.

Conclusions

In south Alaska, δW from lakes in maritime settings closely reflects δP, whereas δW from interior lakes is strongly affected by evaporation. Lakes in the transitional climate setting are also influenced by evaporation, but have generally lower δW values due to colder temperatures at the higher-elevation sites sampled for this study. Meteorological data from the climate station at Whittier in western Prince William Sound show that the majority of precipitation falls during the fall and winter months, when the atmospheric circulation is strongly influenced by the Aleutian Low. Therefore, if regional δP is influenced by the strength and position of the Aleutian Low, δW will likely change as well. The paucity of long-term precipitation collections from south Alaska, however, prevents a rigorous test of this hypothesis.

Mica Lake in western Prince William Sound is not influenced significantly by evaporation, and $\delta^{18}O_{diatom}$

recovered from its lake sediment appears to record δW of water in which diatoms grew. The lack of an overall downcore trend towards higher $\delta^{18}O_{diatom}$ values, combined with diatom assemblage analyses, suggests that non-climatic influences on $\delta^{18}O_{diatom}$ are minimal. The seasonal difference in $\delta^{18}O$ of precipitation collected at Adak is low (+0.4‰), suggesting that the seasonality of precipitation is not an important control on δW. We suggest that changes in the trajectory and frequency of storms intersecting south Alaska is the leading control, which seems most plausible considering the link between the Aleutian Low and wintertime precipitation in south Alaska. We acknowledge that $\delta^{18}O_{diatom}$ values at Mica Lake integrate the effects of multiple controls. Changes between meridional and zonal flow due to the changing position and intensity of the Aleutian Low would likely cause changes of storm trajectories. Under zonal flow conditions, south Alaska would receive isotopically-depleted moisture because of greater rain-out. South-to-north moisture transport over the Gulf of Alaska under meridional flow conditions would cause less rain-out and therefore higher δP.

During the early to mid-Holocene ($\sim$9.6 to 2.6 ka) $\delta^{18}O_{diatom}$ values at Mica Lake are relatively high (+28.6 $\pm$ 0.5‰) and stable. Since $\sim$2.6 ka, brief, episodic decreases in $\delta^{18}O_{diatom}$ suggest more variable atmospheric circulation, which might be linked to large-scale circulation patterns in the North Pacific. Low $\delta^{18}O_{diatom}$ values between $\sim$1700 and 1900 AD coincide with the Little Ice Age, a time of widespread cooling, and glacier expansion in south Alaska. Other times with similarly low $\delta^{18}O_{diatom}$ occurred $\sim$1.3 and 2.3 ka. Results from Mica Lake suggest that the Aleutian Low was weaker and a greater proportion of moisture was delivered by zonal flow during these intervals.

Other δP paleorecords in the northern North Pacific show only weak correlations with air temperature (e.g. Holdsworth et al. 1992; Wake et al. 2002) or have $\delta^{18}O$ variations that are too great to be explained by changes in temperature (e.g. Anderson et al. 2005) and have been interpreted as "source meters" (Fisher et al. 2004). The large variability of $\delta^{18}O_{diatom}$ values from evaporation-insensitive Mica Lake also suggests that the general atmospheric circulation of the North Pacific region has changed on centennial timescales. Viewed collectively, the growing number of δP paleorecords from the North Pacific emphasizes the variability of wintertime storm tracks as a pervasive feature of the climate of northwest North America.

Acknowledgements We thank A. Henderson for his knowledge and assistance with isolating diatoms. N. McKay, T. Daigle, C. Kassel, E. Helfrich, and P. Foletta assisted us in core recovery from Mica Lake and H. Roop and K. Kathan, provided assistance during water sampling. We thank K. Wallace for help with tephra identification and logistical support in Anchorage. D. Fisher provided valuable insight and permission to publish the Mt. Logan data. This project is a contribution to the ARCSS 2 kyr project and was funded by the National Science Foundation (ARC 0455043 and ATM-0318341), the Geological Society of America, the USGS/Alaska Volcano Observatory, and the Natural Sciences and Engineering Research Council of Canada.

References

Ager TA (1998) Postglacial vegetation history of the Kachemak Bay Area, Cook Inlet, south-central Alaska. In: Kelley KD, Gough LP (eds) Geologic studies in Alaska by the US Geological Survey, 1998. US Geological Survey Professional Paper 1615, pp 147–165

Anderson L, Abbot MB, Finney BP, Burns S (2005) Regional atmospheric circulation change in the North Pacific during the Holocene inferred from lacustrine carbonate oxygen isotopes, Yukon Territory, Canada. Quat Res 64:21–35. doi:10.1016/j.yqres.2005.03.005

Beikman HM (1980) Geologic map of Alaska; U.S. Geological Survey Professional Paper PP 0171, 1 plate

Brandriss ME, O'Neil JR, Edlund MB, Stoermer EF (1998) Oxygen isotope fractionation between diatomaceous silica and water. Geochim Cosmochim Acta 62:1119–1125. doi: 10.1016/S0016-7037(98)00054-4

Brewer TS, Leng MJ, Mackay AW, Lamb AL, Tyler JJ, Marsh NG (2008) Unraveling contamination signals in biogenic silica oxygen isotope composition: the role of major and trace element geochemistry. J Quat Sci 23:321–330. doi: 10.1002/jqs.1171

Cayan DR, Peterson DH (1989) The influence of the North Pacific atmospheric circulation on streamflow in the west. Geophys Monogr 55:375–379

Daigle T, Kaufman DS (2008) Holocene climate inferred from glacier extent, lake sedimentation, and tree rings at Goat Lake, Kenai Mountains, Alaska. J Quat Sci (in press). doi: 10.1002/jqs.1166

Dansgaard W (1964) Stable isotopes in precipitation. Tellus 16:436–468

Dodd JP, Sharp ZD, Fawcett PJ, Schiff C, Kaufman DS (2007) A laser-extraction technique for oxygen isotope analysis of diatom frustules. Eos Trans AGU 88(52):B13A–0893

Fisher DA, Wake C, Kreutz K, Yalcin K, Steig R, Mayewski P, Anderson L, Zheng J, Rupper S, Zdanowicz C, Demuth M, Waszkiewicz M, Dahl-Jensen D, Goto-Azuma K, Bourgeois JB, Koerner RM, Sekerka J, Osterberg E, Abbott MB, Finney BP (2004) Stable isotope records from Mount

Logan, Eclipse ice cores, nearby Jellybean Lake. Water cycle of the North Pacific over 2000 years and over five vertical kilometers: sudden shifts and tropical connections. Géographie Physique et Quaternaire 58:9033–9048

Gat JR (1981) Isotopic fractionation. In: Gat JR, Gonfiantini R (eds) Stable isotope hydrology, IAEA Technical Report Series 210. International Atomic Energy Agency, Vienna, Austria, pp 21–33

Gregory-Eaves I, Smol JP, Finney BP, Edwards ME (1999) Diatom-based transfer functions for inferring past climatic and environmental changes in Alaska, U.S.A. Arct Antarct Alp Res 31:353–365. doi:10.2307/1552584

Heegaard E, Birks HJB, Telford RJ (2005) Relationships between calibrated ages and depth in stratigraphical sequences: an estimation procedure by mixed-effect regression. Holocene 15:612–618. doi:10.1191/0959683605hl836rr

Hein MK (1990) Flora of Adak Island, Alaska: Bacillariophyceae (Diatoms). Bibliotheca Diatomologica Band 21. J. Cramer Verlag, Berlin, 133 pp

Heusser CJ (1983) Holocene vegetation history of the Prince William Sound region, south-central Alaska. Quat Res 19:337–355. doi:10.1016/0033-5894(83)90040-6

Hodge SM, Trabant DC, Krimmel RM, Heinrichs TA, March RS, Josberger EG (1998) Climate variations and changes in mass of three glaciers in western North America. J Clim 11:2161–2179. doi:10.1175/1520-0442(1998)011<2161:CVACIM>2.0.CO;2

Holdsworth G, Krouse HR, Nosal M (1992) Ice core climate signals from Mount Logan, Yukon A.D. 1700–1897. In: Bradley RS, Jones PD (eds) Climate since A.D. 500. Routelidge, London, pp 483–516

Hu FS, Ito E, Brown TA, Curry BB, Engstrom DR (2001) Pronounced climatic variations in Alaska during the last two millennia. Proc Natl Acad Sci USA 98:10552–10556. doi:10.1073/pnas.181333798

Juillet A (1980) Structure de la silice biogénique: nouvelles données apportees par l'analyse isotopique de l'oxygène. CR Acad Sci 290:1237–1239

Juillet-Leclerc A, Labeyrie L (1987) Temperature dependence of the oxygen isotope fractionation between diatom silica and water. Earth Planet Sci Lett 84:69–74. doi:10.1016/0012-821X(87)90177-4

Kalnay E, Kanamitsu M, Kistler R, Collins W, Deaven D, Gandin L et al (1996) The NCEP/NCAR 40-Year Reanalysis Project. Bull Am Meteorol Soc 77:437–470. doi:10.1175/1520-0477(1996)077<0437:TNYRP>2.0.CO;2

Lawrence JR, Gedzelman SD, White JWC, Smiley D, Lazov P (1982) Storm trajectories in eastern US D/H isotopic composition of precipitation. Nature 296:638–640. doi:10.1038/296638a0

Leng ML, Barker PA (2006) A review of the oxygen isotope composition of lacustrine diatom silica for palaeoclimate reconstruction. Earth Sci Rev 75:5–27. doi:10.1016/j.earscirev.2005.10.001

Leng ML, Marshall JD (2004) Palaeoclimate interpretation of stable isotope data from lake sediment archives. Quat Sci Rev 23:811–831. doi:10.1016/j.quascirev.2003.06.012

McKay N (2007) Late Holocene climate at Hallet and Greyling Lakes, central Chugach Range, south-central Alaska. M.S. Thesis, Flagstaff, Arizona, Northern Arizona University, 96 pp

Moore GWK, Holdsworth G, Alverson K (2002) Climate change in the North Pacific region over the past three centuries. Nature 420:401–403. doi:10.1038/nature01229

Moore GWK, Alverson K, Holdsworth G (2003) The impact that elevation has on the ENSO signal in precipitation records from the Gulf of Alaska region. Clim Change 59:101–121. doi:10.1023/A:1024423925161

Morley DW, Leng MJ, Mackay AW, Sloane HJ, Rioual P, Battarbee RW (2004) Cleaning of lake sediment samples for diatom oxygen isotope analysis. J Paleolimnol 31:391–401. doi:10.1023/B:JOPL.0000021854.70714.6b

Mortlock RA, Froelich PN (1989) A simple method for the rapid determination of biogenic silica opal in pelagic marine sediments. Deep-Sea Res 36:1415–1426. doi:10.1016/0198-0149(89)90092-7

Moschen R, Lücke A, Parples J, Radtke U, Schlesser GH (2006) Transfer and early diagenesis of biogenic silica oxygen isotope signals during settling and sedimentation of diatoms in a temperate freshwater lake (Lake Holzmaar, Germany). Geochim Cosmochim Acta 70:4367–4379. doi:10.1016/j.gca.2006.07.001

Newman JE, Branton CI (1972) Annual water balance and agricultural development in Alaska. Ecology 53:519. doi:10.2307/1934243

Overland JE, Adams JM, Bond NA (1999) Decadal variability of the Aleutian Low and its relation to high-latitude circulation. J Clim 12:1542–1548. doi:10.1175/1520-0442(1999)012<1542:DVOTAL>2.0.CO;2

Papineau JM (2001) Wintertime temperature anomalies in Alaska correlated with ENSO and PDO. Int J Climatol 21:1577–1592. doi:10.1002/joc.686

Reimer PJ, Baillie MGL, Bard E, Bayliss A, Beck JW, Bertrand CJH et al (2004) INTCAL04 terrestrial radiocarbon age calibration, 0–26 cal kyr BP. Radiocarbon 46:1029–1058

Rings A, Lücke A, Schleser GH (2004) A new method for the quantitative separation of diatom frustules from lake sediments. Limnol Oceanogr Methods 2:25–34

Rodionov SN, Overland JE, Bond NA (2005) Spatial and temporal variability of the Aleutian Climate. Fish Oceanogr 14:3–21. doi:10.1111/j.1365-2419.2005.00363.x

Round FE, Crawford RM, Mann DG (1990) The diatoms: biology and morphology of the genera. Cambridge University Press, Cambridge, 747 pp

Rozanski K, Araguás-Araguás L, Gonfiantini R (1993) Isotopic patterns in modern global precipitation. In: Swart PK, Lohmann KC, McKenzie J, Savin S (eds) Climate change in continental isotopic records. Geophysical Monograph 78. American Geophysical Union, Washington, DC, pp 1–36

Rupper S, Steig EJ, Roe G (2004) The relationship between snow accumulation at Mt. Logan, Yukon, Canada, and climate variability in the North Pacific. J Clim 17:4724–4739. doi:10.1175/JCLI-3202.1

Salathé EP (2006) Influences of a shift in North Pacific storm tracks on western North American precipitation under global warming. Geophys Res Lett 33. doi:10.1029/2006GL026882

Sauer PE, Miller GH, Overpeck JT (2001) Oxygen isotope ratios of organic matter in arctic lakes as a paleoclimate

proxy: field and laboratory investigations. J Paleolimnol 25:43–64. doi:10.1023/A:1008133523139

Schiff CJ (2007) A modern survey and Holocene record of lake water and diatom isotopes from south Alaska. M.S. Thesis, Flagstaff, Arizona, Northern Arizona University, 103 pp

Schiff CJ, Kaufman DS, Wallace KL, Werner A, Ku R, Brown TA (2008) Modeled tephra ages from lake sediments, base of Redoubt Volcano, Alaska. Quat Geochronol 3:56–67. doi:10.1016/j.quageo.2007.05.001

Smol JP, Wolfe AP, Birks HJB, Douglas MSV, Jones VJ, Korhola A et al (2005) Climate-driven regime shifts in the ecology of arctic lakes. Proc Natl Acad Sci USA 102:4397–4402. doi:10.1073/pnas.0500245102

Spooner IS, Barnes S, Baltzer KB, Raeside R, Osborn GD, Mazzuchi D (2003) The impact of air mass circulation dynamics on Late Holocene paleoclimate in northwestern North America. Quat Int 108:77–83. doi:10.1016/S1040-6182(02)00196-9

Stuiver M, Reimer PJ (1993) Extended ^{14}C database and revised CALIB 3.0 ^{14}C calibration program. Radiocarbon 35:215–230

Swann GE, Leng MJ, Sloane HJ, Maslin MA (2008) Isotope offsets in marine diatom δ^{18}O over the last 200 ka. J Quat Sci 23:389–400. doi:10.1002/jqs.1185

Telford RJ, Heegaard E, Birks HJB (2004) The intercept is a poor estimate of a calibrated radiocarbon age. Holocene 14:296–298. doi:10.1191/0959683604hl707fa

ter Braak CJF, Prentice IC (1988) A theory of gradient analysis. Adv Ecol Res 18:271–317. doi:10.1016/S0065-2504(08)60183-X

ter Braak CJF, Smilauer P (1998) CANOCO reference manual and user's guide to Canoco for Windows: software for canonical community ordination (version 4). Microcomputer Power, Ithaca, NY, 352 pp

Trenberth KE, Hurrell JW (1994) Decadal atmosphere-ocean variations in the Pacific. Clim Dyn 9:303–319. doi:10.1007/BF00204745

Vose RS, Schmoyer RL, Steurer PM, Peterson TC, Heim R, Karl TR, Eischeid JK (1992) The global historical climatology network; Long-term monthly temperature, precipitation, sea level pressure, and station pressure data. ORNL/CDIAC-53, NDP-041. Available on-line [http://cdiac.esd.ornl.gov/epubs/ndp/ndp041/ndp041.html] from Carbon Dioxide Information Analysis Center (CDIAC), Oak Ridge National Laboratory, Oak Ridge, Tennessee, USA

Wake CP, Yalcin K, Gundestrup NS (2002) The climate signal recorded in the oxygen-isotope, accumulation and major-ion time series from the Eclipse ice core, Yukon Territory, Canada. Ann Glaciol 35:416–422. doi:10.3189/172756402781817266

Wiles GC, Barclay DJ, Calkin PE, Lowell TV (2008) Century to millennial-scale temperature variations for the last two thousand years indicated from glacial geologic records of Southern Alaska. Global Planet Change 60:115–125. doi:10.1016/j.gloplacha.2006.07.036

Wilson R, Wiles G, D'Arrigo R, Zweck C (2007) Cycles and shifts: 1,300 years of multi-decadal temperature variability in the Gulf of Alaska. Clim Dyn 28:425–440. doi:10.1007/s00382-006-0194-9

Wolfe AP (2002) Climate modulates the acidity of arctic lakes on millennial timescales. Geology 30:215–218. doi:10.1130/0091-7613(2002)030<0215:CMTAOA>2.0.CO;2

Wooller MJ, Francis D, Fogel ML, Miller GH, Walker IR, Wolfe AP (2004) Quantitative paleotemperature estimates from δ^{18}O of chironomid head capsules preserved in arctic lake sediments. J Paleolimnol 31:267–274. doi:10.1023/B:JOPL.0000021944.45561.32